Bull. Chem. Soc. Jpn., 73, 1525—1533 (2000)

Electronic Spectra of Push-Pull 4-Phenylaminoazobenzene Derivatives

Shohei Makita, Ayako Saito, Makoto Hayashi, Shohei Yamada, Koji Yoda, Joe Otsuki, Toshio Takido, and Manabu Seno*

Department of Materials and Applied Chemistry, College of Science & Technology, Nihon University, 1-8-14 Kanda Surugadai, Chiyoda-ku, Tokyo 101-8308

(Received December 1, 1999)

A series of push-pull type 4-phenylaminoazobenzene derivatives bearing an electron-withdrawing 4′-substituent were probed by electronic spectra in solution. The visible absorption maxima of these azobenzenes were correlated with the solvent parameters through the McRae theory as well as the solvent donor numbers. While the absorption spectra of these neutral species were solvent-dependent, those of protonated species were almost solvent independent. On the other hand, the absorption maxima and the rates of thermal *cis*-to-*trans* isomerization in a given solvent were correlated with Hammett constants. These results are discussed with the help of semi-empirical molecular-orbital calculations and compared with previously published data on related compounds.

Aromatic azo compounds have been known for a long time and still constitute active areas of investigation, in view of both their basic interest and their potential applications. Photochromism,[1—3] protonation behavior,[4] and redox activity[5,6] are the main features of their interest. Further, recently in particular, push-pull type azobenzene derivatives, which have an electron-donating group on one end and an electron-withdrawing group on the other, are being widely used as non-linear optic materials.[7] We noticed, however, that basic data were lacking for some kinds of compounds. 4-Phenylaminoazobenzene derivatives were one of those classes of compounds whose systematic data are missing in literature. In most studies treating 4-phenylaminoazobenzene (**1**) and 4-nitro-4′-phenylaminoazobenzene (**3**), these compounds have been compared with other amino or alkylamino derivatives.[8—12] In opposition to these previous studies, we kept the 4-phenylamino group invariant and examined the effect of a variety of 4′-substituents with electron-withdrawing propensity. The entries in this study, **1**—**8**, are shown in Chart 1. The electronic spectra were used to probe substituent and solvent effects, the protonation behavior, and photochromism.

Results

Substituent and Solvent Effects. The electronic spectra of **1**—**8** were measured in some representative solvents. Two absorption bands were observed: one around 270 nm and the other around 450 nm. The latter absorption bands are tabulated in Table 1. While the shorter wavelength absorption band remains virtually unaltered in different solvents, the longer wavelength absorption is solvent-dependent, and ranges from 420 nm in $CHCl_3$ to 492 nm in DMSO. Another way of viewing Table 1 is to examine the substituent effects by comparing λ_{max} for different compounds in the same solvent. For example, in MeOH, the lower energy absorption band ranges from 408 nm for **1** with no 4′-substitution to 466 nm for 4′-nitro-substituted **3**, having the strongest electron-withdrawing group.

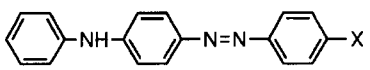

1 (X = H), **2** (X = CN), **3** (X = NO_2), **4** (X = CO_2H), **5** (X = CO_2Me), **6** (X = CO_2Et), **7** (X = $CONH_2$), **8** (X = $CSNH_2$)

Chart 1.

Protonation. Protonated samples were prepared by successively adding aliquots of aqueous HCl to a 25 μM azobenzene solution (1 M = 1 mol dm^{-3}) in MeOH/H_2O (9/1 (v/v)) (3 mL); each addition was followed spectroscopically. All titrations were repeated twice, and every point agreed within ±1% in absorbance. A representative example of this titration is shown in Fig. 1 for **1**. An isosbestic point was measured at 467 nm, which implied that a simple protonation reaction was taking place. The band at 538 nm increased along with a concomitant decrease in the bands at 410 and 270 nm. The newly appeared band is ascribed to the azonium cation (Chart 2), while the absence of a band around 330 nm, which is diagnostic of the ammonium cation,[10] in the spectra of protonated species indicates that the protonated species are almost exclusively azonium cations. This is true for all other compounds, except perhaps for **3**, for which a very small, but noticeable, absorption band is observed at around 330 nm.

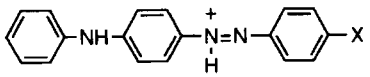

Chart 2.

Table 1. The Electronic Spectra of **1**—**8** in Several Solvents at 25 °C

	$CHCl_3$		EtOAc		THF		MeOH		MeCN		DMSO	
	λ_{max}	$\varepsilon\times10^{-4}$	λ_{max}	$\varepsilon\times10^{-4}$	λ_{max}	$\varepsilon\times10^{-4}$	λ_{max}	$\varepsilon\times10^{-4}$	λ_{max}	$\varepsilon\times10^{-4}$	λ_{max}	$\varepsilon\times10^{-4}$
	nm	$cm^{-1}M^{-1}$	nm	$cm^{-1}M^{-1}$	nm	$cm^{-1}M^{-1}$	nm	$cm^{-1}M^{-1}$	nm	$cm^{-1}M^{-1}$	nm	$cm^{-1}M^{-1}$
1	397	2.7	404	3.1	410	3.4	408	3.1	404	2.9	422	2.6
2	429	3.2	436	3.3	442	3.3	444	3.4	438	3.7	464	3.0
3	450	3.0	456	3.0	464	3.1[a]	466	3.2	455	3.1	492	2.9
4	—[b]	—[b]	424	3.1	432	3.5	424	3.2	426	3.0	448	3.2
5	420	3.1	428	2.9	434	3.3	434	3.6	426	3.2	452	2.8
6	420	2.9	426	3.2	434	3.4	434	3.9	425	2.8	454	3.0
7	418	2.3	419	3.3	424	3.2	428	3.4	420	3.2	442	3.0
8	432	2.6	432	3.2	426	3.4	438	3.3	434	3.2	459	2.9

a) For **3**, the spectra were taken also in the following solvent (solvent, λ_{max} (nm), $\varepsilon\times10^{-4}$ ($cm^{-1}M^{-1}$)): benzene, 448, 2.8; Et_2O, 453, 3.0; pyridine, 488, 2.8; acetone, 462, 2.8; EtOH, 475, 2.1; DMF, 482, 2.9. b) Poorly soluble.

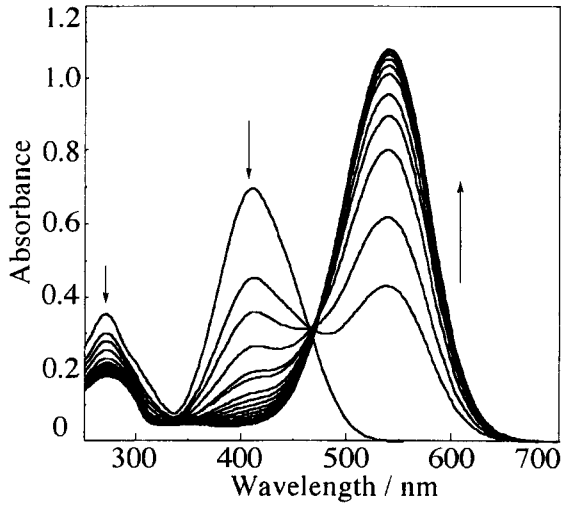

Fig. 1. The spectral changes upon addition of aqueous HCl to a solution of **1** in $MeOH/H_2O$ at 25 °C.

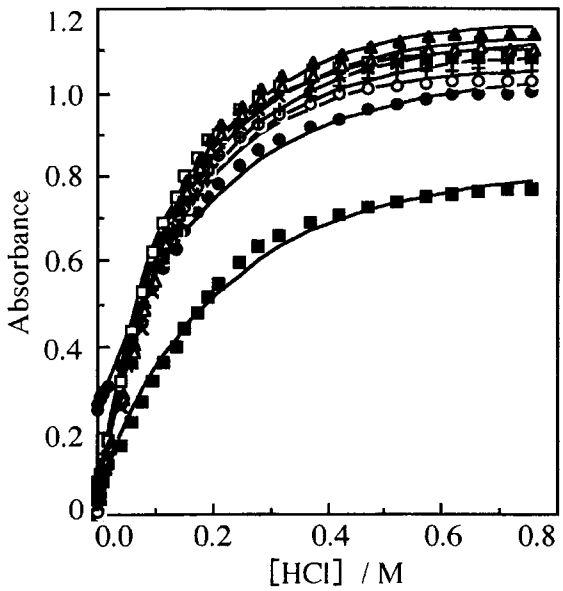

Fig. 2. Titration curves of azobenzenes, **1**—**8**, with aqueous HCl in $MeOH/H_2O$ at 25 °C. The vertical axis represents the absorbance at the λ_{max} of respective protonated species shown in Table 2. Calculated curves are superimposed on observed points (see test): **1** (□), **2** (■), **3** (●), **4** (○), **5** (▲), **6** (△), **7** (×), and **8** (+).

The case of compound **4** having a carboxyl group is worth mentioning. The λ_{max} at 422 nm shifted to 436 nm upon the addition of the first aliquot, 6 μL of 1 M aqueous HCl, in the titration. The shift is evidently due to H^+ and/or Cl^- ions, and thus specific solute–ion interactions occur around the carboxyl group. The possibility of protonation or azonium formation as the cause of this initial shift can be excluded on the basis that a different peak at 538 nm, characteristic of the protonated species, gradually developed with an isosbestic point upon further addition of aqueous HCl.

These spectral changes were plotted against the added amount of HCl, as shown in Fig. 2. A least-squares curve fitting procedure, assuming the formation of a protonated species of azobenezene : HCl = 1 : 1 stoichiometry, gives calculated curves which are superimposed on the observed absorbances. The association constants, K = [azobenzene-HCl]/[azobenzene][HCl], obtained in the curve-fitting procedure are tabulated in Table 2. The values of K for **1**—**8** are all of the same order of magnitude. Still, the order of magnitude is as expected (**1** > **4**,**5**,**6**,**7**,**8** > **2**,**3**), and roughly correlates with the electron-withdrawing strength of the substituents. Slight, but consistent, deviations of the calculated curve from the observed points can be noted in Fig. 2. This is most likely attributed to medium changes during titration. It should be mentioned that the composition of the medium changed from $MeOH/H_2O$ = 90/10 at the beginning to $MeOH/H_2O$ = 77/23 at the end of titration. Probably more important is that, since nearly a molar amount of acid was present in large excess toward the end of the titration, ion pairs formed should have been solvated by the molecules of the acid. Widernik et al. reported that the protonation reactions of **1** in 1,4-dioxane, MeCN, and $MeNO_2$ run according to the following scheme involving two molecules of acid (AH) : azobenzene+$(AH)_2$ ⟺ (azobenezene$(AH)_2$).[10] This scheme should lead to a sigmoidal curve, which is clearly not the case here.

Table 2 also includes λ_{max}'s and ϵ's of the spectra at the

Table 2. The Association Constants with HCl and the Electronic Spectra of **1**—**8** in Their Protonated States in MeOH/H_2O

	K / M^{-1}	λ_{max} / nm	$\varepsilon \times 10^{-4}$ / $cm^{-1}M^{-1}$
1	7.9	538	5.0
2	3.4	531	3.6
3	3.6	533	4.6
4	6.6	537	4.8
5	6.3	538	5.3
6	6.3	538	5.1
7	5.9	539	5.0
8	5.9	550	4.9

end of the titration, where the protonation is practically complete. A striking feature is that, while the λ_{max} of the neutral species depends strongly on the 4′-substituent, those of the protonated species do not.

It was previously noted that introducing the *N*-phenyl substituent makes the ammonium form disappear, while both tautomers are observed for 4-aminoazobenzene and its *N*-alkyl and *N*,*N*-dialkyl derivatives.[10] Here, it is confirmed that this is also the case for the push-pull type *N*-phenyl derivatives, although a very small amount of ammonium cation may exist for **3**, as described above.

Photochromism. Changes in the electronic spectra upon photo-irradiation and during a subsequent dark reaction for **2** in MeCN are shown in Fig. 3 as an example. The isosbestic points expected for a simple isomerization were observed during photobleaching and recovery in each case; in the case of the example shown in Fig. 3, isosbestic points were found at 323, 378, and 536 nm. All photoirradiated azobenzenes restored the original color nearly completely after being kept in the dark. Repeated irradiation to these samples resulted in identical spectral changes with those by the first irradiation.

The rate of the reverse dark reaction followed the expected first-order kinetics: $[cis] = [cis]_0 \exp(-kt)$, where $[cis]_0$ is the concentration of *cis* form at the photostationary state and k is the rate constant. The rate constants, obtained by fitting the experimental absorbance changes to the equation, are summarized in Table 3. The excellent fit of the first-order kinetics of the thermal *cis*–*trans* isomerization to the observed

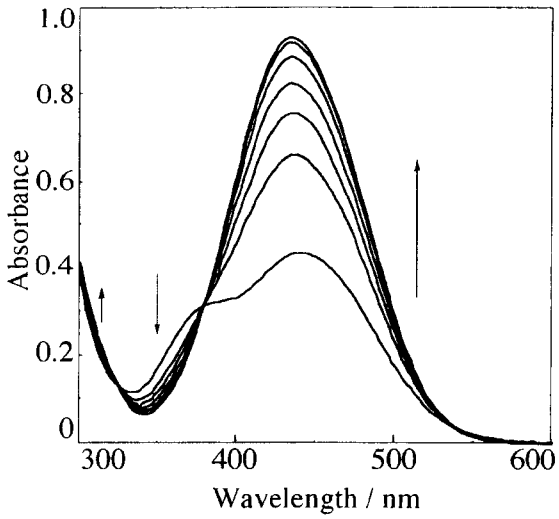

Fig. 3. Thermal recovery process of **2** (25 μM) in MeCN from the photostationary state at 25 °C. The bottom spectrum around 450 nm is of photostationary state, while the completely recovered spectrum at the top coincides with that before photoirradiation.

absorbance changes confirms that the original spectra before irradiation were indeed those of pure *trans* form.

It is known that the *cis* isomer shows two absorption bands, one on the long-wavelength edge and the other on the short-wavelength edge of the visible absorption band of the *trans* isomer.[8,13] There is a wavelength region between these two bands where the extinction coefficient is practically zero. From the spectrum of the photostationary state in Fig. 3, it is most likely that this minimum absorption region is around 400 nm. Incidentally, the minimum absorption appears at the same 400 nm for all compounds studied in any solvent. Hence, it was assumed that absorption by the *cis* form at 400 nm is negligible for the determination of the quantum yields, $\phi_{t\to c}$, of *trans*-to-*cis* photoisomerization. Thus, the obtained values should be regarded as the lower limits. However, residual absorption by the *cis* isomer would not cause a large error, unless the absorption at the photostationary state approaches near zero, which was not the case. At the photostationary state, the reaction rate from *trans* to *cis* must be equal to that of the reverse reaction,

Table 3. The Quantum Yields of *trans*-to-*cis* Photoisomerization and the Rate Constants of *cis*-to-*trans* Thermal Isomerization at 25 °C

	THF		MeCN		DMSO	
	$\phi_{t\to c}$	$k \times 10^5/s^{-1}$	$\phi_{t\to c}$	$k \times 10^5/s^{-1}$	$\phi_{t\to c}$	$k \times 10^5/s^{-1}$
1	0.007	5.8	0.007	4.8	0.004	5.4
2	0.014	58.4	0.032	88.8	0.011	382
3	—[a]	—[a]	—[a]	—[a]	—[a]	—[a]
4	0.005	10.2	0.014	30.8	0.005	17.5
5	0.008	17.0	0.007	10.2	0.011	82.0
6	0.007	13.3	0.006	9.4	0.008	58.0
7	0.005	7.6	0.006	7.6	0.007	22.7
8	—[a]	—[a]	0.036	75.7	0.006	37.7

a) The quantum yield and the rate constant could not be determined, since photoirradiation did not cause an spectral change from the initial dark-adapted state.

$$I_0(1-10^{-A})\phi_{t\rightarrow c} = k[cis]_0 N(V/1000),$$

where I_0 (8.0×10^{14} quanta s^{-1}) is the light intensity, A the absorbance at 400 nm, N Avogadro's constant, and V (3 mL) the sample volume in mL. The results obtained by the above equation are given in Table 3. The estimated errors are $\pm10\%$, mostly due to fluctuation in the light intensity.

Discussion

Substituent Effect. Organic aromatic azo compounds are grouped into three types, according to Dürr and Bouas–Laurent, by the relative energetic position of the $^1(n,\pi^*)$- and the $^1(\pi,\pi^*)$-states.[1] These are the azobenzene type, characterized by a large (π,π^*)–(n,π^*) state gap; the aminoazobenzene type, characterized by close-lying $^1(n,\pi^*)$- and $^1(\pi,\pi^*)$-states; and the pseudo stilbene type, characterized by a low-lying $^1(\pi,\pi^*)$-state. The azobenzene derivatives dealt here are in either one of the latter two groups. Compound **1** with no substituent on carbon-4′ is of the aminoazobenzene type; **2** and **3** with a strong electron-withdrawing group on carbon-4′ are in the pseudo stilbene type; and the others are of intermediate character of the two groups. Thus, the absorption band at around 450 nm is due to a mixed (π,π^*) and (n,π^*) transition, the former transition being, naturally, predominant in intensity.[14]

To gain insight into the nature of these transitions, ZINDO calculations were conducted for **1**—**8**; some of the results are presented in Fig. 4. In the case of **1**, the HOMO consists mainly of the p_z-orbitals of amino nitrogen and carbon-1 adjacent to the azo nitrogen. The LUMO largely consists of the p_z-orbitals of both azo-nitrogens. Thus, the transition is (π,π^*), with a charge-transfer character. In the case of **3**, while a large part of the HOMO remains on the amino nitrogen, contributions from some of the p_z-orbitals of carbons designated in Fig. 4 are apparent. The LUMO of **3** is pulled into, and more delocalized over, the whole nitrobenzene moiety, and hence of lower energy than that of **1**. Thus, the transition is (π,π^*), with a larger charge-transfer nature than that of **1**. For other azobenzenes containing an electron-withdrawing group less powerful than the nitro group, **2** and **4**—**8**, the HOMOs are more or less the same, and lie mainly on the amino nitrogen. The extent of delocalization of LUMO is dependent on the 4′-substituent, and is reflected in the energy and, consequently, the absorption spectra.

Some relation between the observed λ_{max} and the polar characteristics of the substituent is thus expected. The values of λ_{max} are plotted against the Hammett constants, σ_P, for the 4′-substituents (Fig. 5). It is clear that the Hammett parameters correlate nearly linearly with the observed λ_{max}'s in various solvents. A linear dependence was also observed for a series of substituted 4-[(2-cyanoethyl)(2-hydroxyethyl)amino]-2-methylazobenzenes and substituted 4-[(2-cyanoethyl)amino]-2-methylazobenzenes in EtOH.[15]

Solvent Effect. We examined several representative parameters characterizing the solvent properties that might possibly account for the observed solvatochromic shifts. The examined parameters included the dielectric constants, dipole moments, Kosower's Z-values, E_T-values by Dimroth and Reichardt, acceptor numbers, and donor numbers (D_N).[16] We found that the observed shifts show a correlation only with D_N among these parameters. A general trend can be

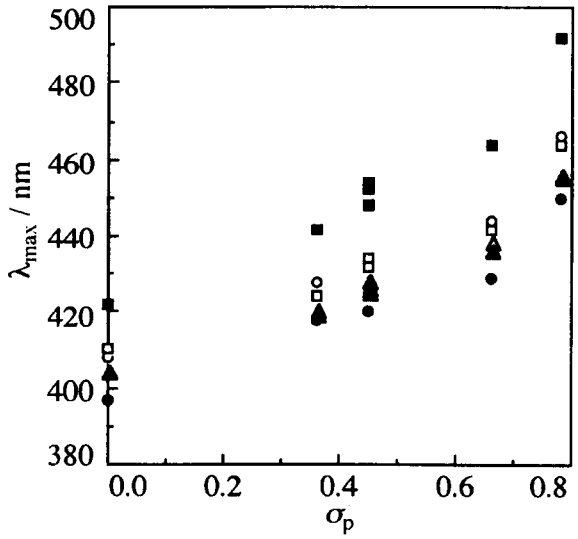

Fig. 5. The Hammett relationship between λ_{max} and σ_P: $CHCl_3$ (●), EtOAc (▲), THF (□), MeOH(○), MeCN (△), and DMSO (■).

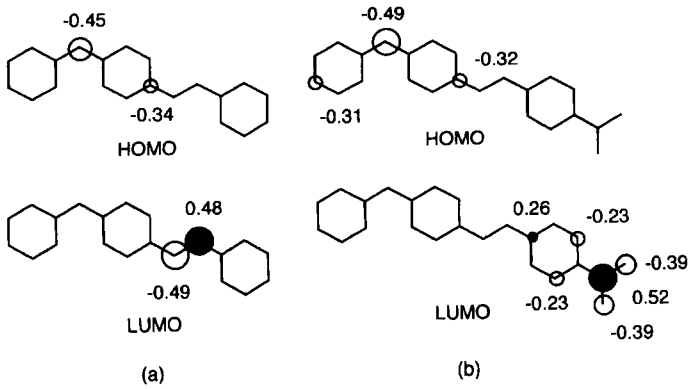

Fig. 4. The HOMO and LUMO of **1** (a) and **3** (b). Only major contributions are shown for clarity. Black and white circles show the phase of the molecular orbitals. The numbers are the expansion coefficients of the p_z-orbitals of atomic orbitals used as the bases set.

seen from the data in Table 1 that the λ_{max} is smaller in solvents of larger D_N. To confirm this observation, the spectra were taken in an extended series of solvents for **3** (footnote a) of Table 1), and the values of λ_{max} were plotted against the D_N of solvents as shown in Fig. 6. A clear relationship between λ_{max} and D_N can be seen from the graph, although there are some scattered points in the plot. That the D_N value correlates with the transition energy suggests that the solute azobenzene apparently behaves as a hard acceptor. The relevant interaction site is, most probably, the amino hydrogen commonly present in **1**—**8**. In the transition process manifested in the absorption spectra, the negative charge transfers from the amino nitrogen, on which a major part of the HOMO localizes, to the benzene ring bearing an electron-withdrawing substituent, where the LUMO lies. Therefore, a positive charge should develop at the amino nitrogen in the excited state. The fact that the transition energy shifts to a lower wavenumber in solvents of larger D_N suggests that the developed charge in the excited state is stabilized more in solvents of larger D_N. The Franck–Condon principle argues that the solvent molecules around the solute molecule cannot change their orientation during the transition. This leads to the conclusion that the orientation of (a) solvent molecule(s) interacting with the amino moiety in the ground state is also favorable in the excited state.

It is interesting to examine the effect of amino hydrogen in this stabilizing effect. The transition energies of 4-diethylamino-4′-nitroazobenzene, which lacks a hydrogen atom on the amino nitrogen, in various solvents are available.[17] We plotted these values against D_N, which is also shown in Fig. 6. The points are somewhat more scattered compared with those of **3**, although the general trend is more or less similar to those for **3**. If a linear correlation is assumed, the correlation coefficients are 0.75 and 0.36 for **3** and 4-diethylamino-4′-nitroazobenzene, respectively. That a better correlation has been found for **3** than for the diethylamino derivative may suggest a role of amino hydrogen in mediating donating properties of the solvent molecules to stabilize the positive charge developed on the amino nitrogen.

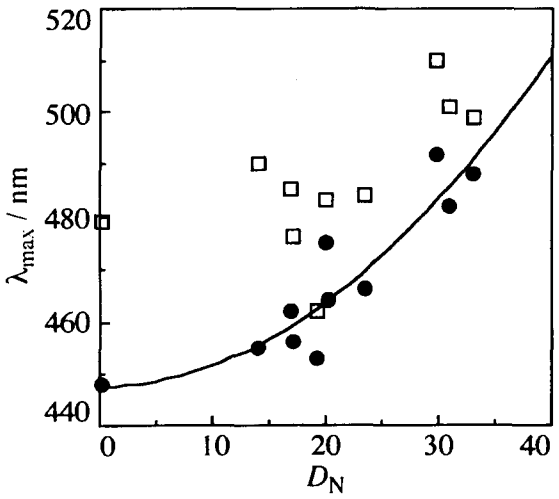

Fig. 6. The relationship between λ_{max} and D_N of solvents for **3** (●) and 4-diethylamino-4′-nitroazobenzene (□).[17] Studied solvents are (solvent, D_N[16]): benzene, 0.1; MeCN, 14.1; acetone, 17.0; EtOAc, 17.1; Et_2O, 19.2; EtOH 20; THF, 20.1; MeOH, 23.5; DMSO, 29.8; DMF, 30.9; pyridine, 33.1.

The effects of electronic dipole interactions on the electronic band frequencies in solution spectra were analyzed theoretically by McRae.[18] An approximate form of the McRae equation gives the frequency shift, $\Delta\nu$, of a compound as follows:

$$\Delta\nu = (AL_0 + B')\frac{n_D^2 - 1}{2n_D^2 - 1} + C\left[\frac{D_s - 1}{D_s + 2} - \frac{n_D^2 - 1}{n_D^2 + 2}\right],$$

where n_D is the solvent refractive index and D_S is the static dielectric constant of the solvent. A, B', and C are parameters related to the solute, and L_0 is to the solvent. This equation was derived by applying a second-order perturbation treatment to a solute dipole in solvent dipoles interacting among them. The frequency shift is thus the sum of the contributions from dispersive and static dipole interactions.

Irick and Pacifici found that the observed frequency shifts are satisfactorily explained by the above equation for 4-diethylamino-4′-substituted azobenzenes.[17] They used values of -25.030 and -2.171 cm^{-1} for AL_0+B' and C, respectively. We superimposed our data set in Table 1 on the graph of Irick and Pacifici, which is shown in Fig. 7. Hexane was employed as the reference solvent in determining the frequency shift. Since the absorption frequency in hexane was not available for our compounds, due to a solubility problem, except for **1**, this is set to be the best fitting value for each compound. The estimation from the above treatment predicts the λ_{max} for **1** in hexane as 384 nm, which is exactly as measured (λ_{max} = 384 nm, $\varepsilon = 3.2\times10^{-4}$ cm^{-1} M^{-1}).

It is noted that the fitting is, at best, moderate, although the McRae theory is evidently capable of reproducing the gross features of the phenomena. The deviations are indicative of the presence of some specific solute–solvent interactions, e.g. hydrogen bonding, which are not explicitly included in the

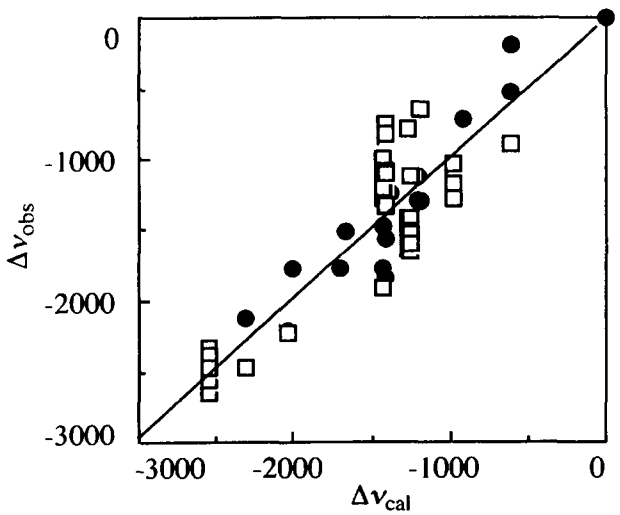

Fig. 7. McRae plot: calculated wavenumber shifts vs. observed shifts: this work (□), Irick, Jr., and Pacifici (●).[17]

McRae treatment and are related to the above argument on D_N. It is remarkable, however, that we have used a single set of parameters: the above-mentioned values for AL_0+B′ and C for all the range of compounds **1**—**8**, and 4-diethylamino-4′-azobenezene. As mentioned above, A, B, and C are constants characteristic of the solute and should reflect solute properties such as the dipole moment vectors of the ground state and excited state. The fact that the common values for these parameters can be used to reproduce the observed frequency shifts implies that these values are insensitive, or tolerant in other words, to the structural or electronic variations seen in these compounds. Although this makes these parameters less useful to predict solute properties, they are more useful in predicting frequency shifts for a range of compounds in various solvents, to an extent.

Protonation. Protonation reactions of 4-aminoazobenzenes and its *N*-substituted derivatives have a long history of investigation.[10—12,20,21] In these early studies, many resonance structures were usually invoked to explain the observed spectra. In order to interpret the spectra from a quantum mechanical viewpoint,[10c] ZINDO calculations were conducted on the azonium cations of **1** and **3**. A proton was assumed to be attached on the azo nitrogen far from the phenylamino group (N^{β}). This is based on the previously shown preference of N^{β} protonation.[10c] In the case of the azonium of **1**, it is shown that the HOMO lies mainly on the amino nitrogen with increased contributions from some carbons in the phenyl ring, as shown in Fig. 8. The LUMO lies on the azo nitrogens again with increased contributions from some carbons in the benzene ring. The partial charges were also calculated and atoms bearing substantial positive or negative net charges are also indicated in Fig. 8. The large bathochromic shift upon azonium formation can be interpreted to be due to the stabilization of LUMO, since the LUMO distributes on the positively charged atoms.

The HOMO and LUMO of protonated **3** are remarkably similar to those of protonated **1**, as shown in Fig. 8. Thus, even a strong electron-withdrawing substituent as a nitro group has little effect on the molecular orbitals of the protonated species. The partial charge distributions for protonated **1** and **3** are also nearly identical, except, of course, for the local charges on the nitro group. These results indicating that the 4′-substituent has little effect on the HOMO, LUMO, and the charges may account for the observed insensitivity of λ_{max} on 4′-substituents, as displayed in Table 2.

Photochromism. Nishimura et al. studied the thermal *cis*-to-*trans* isomerization of substituted azobenzenes, and found that the plot of the rate constants in logarithmic scale against Hammett σ is V-shaped with the minimum near σ equal to zero for *mono* substituted azobenzenes in non-polar solvents.[19] Qualitatively, it is also the case for our data set in Table 3 that the larger is the Hammett constant, the larger is the rate (k) of thermal recovery to the *trans* form. However, the curves of $\log k$ vs. Hammett constants are somewhat scattered, as shown in Fig. 9. For example, the Hammett constants for $-CO_2H$ and $-CO_2Me$ are the same, 0.45, but the rates are not the same for **4** and **5** in any of the solvents studied.

In some cases, no *cis* formation was detected. This is most likely due to very fast *cis*-to-*trans* isomerization. It was already reported that the rate is accelerated for *para*-donor/*para*′-acceptor-substituted azobenzenes, such as 4-dimethylamino-4′-nitroazobenzene, for which the rate is reported to be 120 s^{-1} in DMSO at 25 °C.[19a] Other previously reported relevant values include 2×10^{-3} and 2.7 s^{-1} for **3** in benzene and acetone, respectively, at 25 °C.[8] Another indication of the complexity beyond a simple Hammett relationship is that, while the rates for **1** with no substituent are

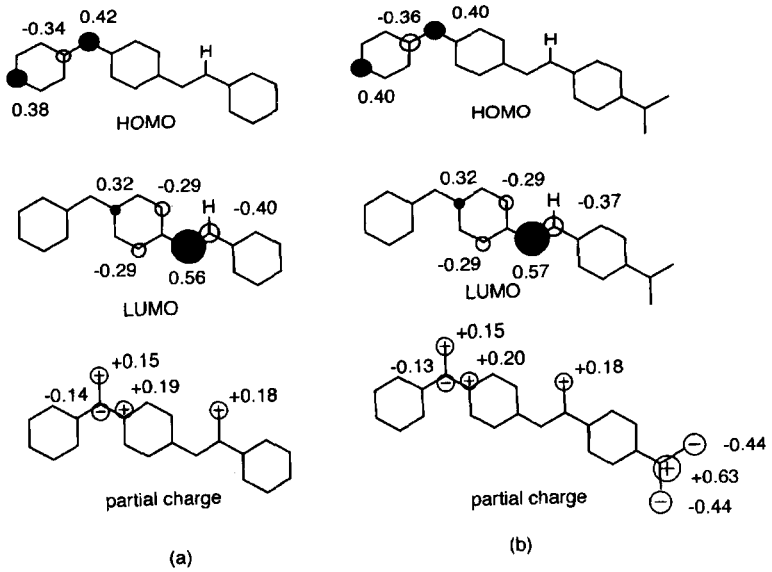

Fig. 8. The HOMO and LUMO of protonated **1** (a) and protonated **3** (b), and partial charges. Only major contributions are shown for clarity. Black and white circles show the phase of the molecular orbitals. The numbers by the orbitals are the expansion coefficients of the p_z-orbitals of atomic orbitals used as the bases set and those by the plus or minus signs are the partial charges.

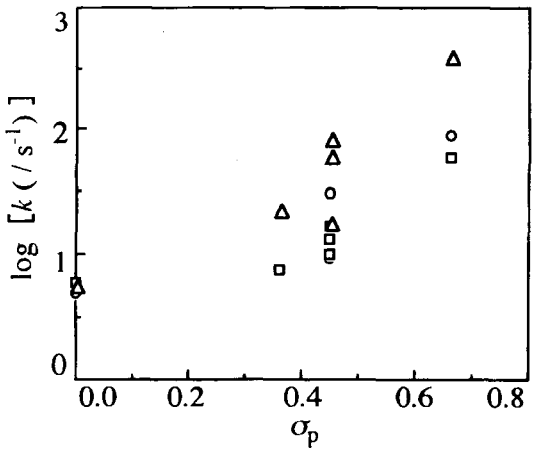

Fig. 9. The Hammett relationship of the rate of thermal *cis*-to-*trans* isomerization reaction at 25 °C: THF (□), MeCN (○), and DMSO (△).

hardly affected by solvents, 4′-substituted derivatives exhibit a strong dependence on the solvent used.

Esters **5** and **6** and amide **7** are similar in behavior, that is, the recovery rates are in the order DMSO > MeCN > THF, which is in accordance with the order of the dielectric constants. However, in stark contrast to this trend is the rate of thioamide **8**. No *cis* formation was observed for **8** in THF in our experimental set up, suggesting that the thermal recovery from *cis*-**8** is very fast ($\gg 400\times10^{-5}$ s^{-1}). This makes the order of recovery rates just reversed from above: THF > MeCN > DMSO. Molecular-orbital calculations on **8** imply no unusual points compared with amide **7**.

The quantum yields of *trans*-to-*cis* photoisomerization when excited by 400 nm light are also given in Table 3. All of the values are more or less on the order of 10^{-2} under the conditions used. The high quantum yield of the azobenzene bearing the second strongest electron-withdrawing cyano group **2** is distinguished. It is unfortunate that the quantum yield for the one with the strongest electron-withdrawing nitro group **3** could not be determined, since the absorption spectrum showed no change upon irradiation. Another point to note is that the quantum yield for the thioamide **8** in MeCN is unusually high. This reactivity of the thioamide derivative, together with the peculiar behavior in the thermal isomerization, needs further scrutiny.

Conclusions

The data are presented on the absorption spectra for a series of 4-phenylaminoazobenzene derivatives bearing electron-withdrawing groups on carbon-4′. It has been shown that the λ_{max} values correlate with the Hammett constants for the para substituent. The solvent dependency can be expressed as dipole–dipole interaction terms through the McRae treatment. It has also been found that the λ_{max} values are correlated with D_N of the solvents. While the λ_{max}'s of neutral azobenzenes shift greatly depending on the solvent, those of azonium cations are exhibited in a narrower wavelength range. Although some of these behaviors were known for other series of push-pull type azobenzenes for a long time, it was attempted here to interpret some of these aspects with the help of modern molecular-orbital calculations.

As for photochromism, there is still an unsettled controversy concerning the mechanism of the thermal isomerization of azobenzene derivatives.[1] Two mechanisms are proposed: inversion of one or both of the nitrogens through a linear (sp hybridized) transition state and rotation about the N=N bond. Although the substituent and solvent dependencies presented here do not lend support to either one preferably over the other, a greater accumulation of data is desirable to sort out factors that affect the rate of thermal isomerization. The apparent unusual behavior, such as that found for **8**, implies that unraveled mechanisms remain for this deceptively simple, old reaction.

Experimental

The electronic spectra were recorded on a Shimadzu UV-2200. All electronic spectra reported in this paper were of a 25 μM solution taken at 25 °C. Sample solutions were stored in a dark place for a time long enough (typically, overnight) prior to the measurement in order to ensure that the species in the sample solution took the pure *trans* form. That the samples prepared as such were indeed of pure trans was confirmed by following the recovery process after photoirradiation (see Photochromism section in Results). For determining of the thermal *cis*-to-*trans* rate constants, light from a 300 W high-pressure Hg lamp was filtered through a Toshiba B-46 filter, which has a transmittance maximum at 460 nm and a half width of 120 nm. The sample was kept at 25 °C by circulating water during photoirradiation and thermal isomerization. For the quantum-yield determination of *trans*-to-*cis* photoisomerization, a 3 mL of 25 μM sample solution was placed in a cell holder, kept at 25 °C by circulating water, in a Hitachi F-2000 fluorescence spectrophotometer, and 400-nm light was irradiated using the 10-nm slit. Irradiation was continued until the photostationary state was reached (several minutes). The light intensity was measured by ferrioxalate actinometry.[22] The flux rate was 8.0×10^{14} quanta s^{-1} on the sample. All solvents used in the measurements of electronic spectra were of spectroscopic grade obtained from Kanto Chemicals and used as received.

Semiempirical ZINDO calculations were carried out using a Sony Techtronics CAChe software. Calculations of the molecular orbitals were conducted with the restricted Hartley–Fock method using INDO/1 parameters and configuration interaction Level 9 on geometry-optimized structures by ZINDO energy minimization.

Syntheses. Melting points were taken on a Yanaco MP500D apparatus. IR spectra were recorded on a Shimadzu FTIR-8100 spectrometer using KBr pellets. ^{1}H NMR spectra were taken on a JEOL JNM-GX400 in $(CD_3)_2CO$ as the solvent, using TMS as an internal standard. Measurements of ^{1}H NMR, microanalysis, and mass spectra were carried out by the Chemical Analysis Center of Nihon University.

Azobenzene derivatives **1**—**4** were prepared according to a standard diazotization–diazonium coupling scheme. A drop of concd HCl was added to a solution of diphenylamine (4.22 g, 25 mmol) in MeOH (60 mL) to adjust its pH to 5—6, as judged by pH paper. Solid $NaNO_2$ was added by portions to a stirred solution of 4-substituted aniline (25 mmol) in concd HCl (8 mL) and H_2O (20 mL) cooled in an ice-bath. To this cooled diazonium salt solution was added the previously prepared solution of diphenylamine, and the mixture was stirred for 3 h at 0—5 °C. The resulting solid was

collected on a filter paper, washed by H_2O, and crystallized from the designated solvent.

1. (Orange plates from hexane, 4.36 g, 64%), mp 90—91 °C (lit,[23] 89—91 °C).

2. (Red needles from EtOH, 5.73 g, 77%), mp 187—188 °C. ^{1}H NMR δ_H = 7.07 (t, 1H, J = 7.2 Hz), 7.25 (d, 2H, J = 9.4 Hz), 7.31 (d, 2H, J = 7.7 Hz), 7.38 (t, 2H, J = 7.7 Hz), 7.92 (d, 2H, J = 8.8 Hz), 7.95 (d, 2H, J = 8.8 Hz), 7.99 (d, 2H, J = 8.8 Hz), 8.03 (br s, 1H). IR (KBr) 3346, 2224, 1599, 1589, 1533, 1495, 1427, 1392, 1348, 1136, 856, 750, 698, 563 cm^{-1}. HRMS (EI 70 eV) Found: *m/z* 298.1244, Calcd for $C_{19}H_{14}N_4$: M, 298.1218. Found: C, 76.42; H, 5.01; N, 18.89%. Calcd for $C_{19}H_{14}N_4$: C, 76.49; H, 4.73; N, 18.78%.

3. (Deep blue crystals from EtOH, 4.77 g, 63%), mp 161—162 °C (lit,[24] 158—159 °C).

4. (Golden plates from EtOH, 5.27 g, 70%), mp 247—249 °C (lit,[25] 250 °C).

5. A suspension of **4** (3.17 g, 10 mmol) and $SOCl_2$ (3.57 g, 30 mmol) in benzene (250 mL) was refluxed for 3 h. To the residue obtained by evaporating excess $SOCl_2$ and benzene, triethylamine (3.03 g, 30 mmol) and MeOH (200 mL) were added and the mixture was refluxed for 2 h. The solvent was evaporated and the resulting residue was dissolved in $CHCl_3$, washed with H_2O, dried over Na_2SO_4, and crystallized from benzene to yield dark-red columnar crystals (2.59 g, 80%), mp 186—188 °C. ^{1}H NMR δ_H = 3.93 (s, 3H), 7.05 (t, 1H, J = 7.7 Hz), 7.25 (d, 2H, J = 8.8 Hz), 7.30 (d, 2H, J = 7.1 Hz), 7.37 (t, 2H, J = 7.2 Hz), 7.92 (d, 2H, J = 8.8 Hz), 7.94 (d, 2H, J = 7.7 Hz), 8.17 (d, 2H, J = 8.8 Hz), 8.24 (br s, 1H). IR (KBr) 3352, 1705, 1589, 1533, 1495, 1431, 1396, 1348, 1286, 1236, 1136,1097, 746, 696 cm^{-1}. HRMS (EI 70 eV) Found: *m/z* 331.1287. Calcd for $C_{20}H_{17}N_3O_2$: M, 331.1321. Found: C, 72.81; H, 5.36; N 12.49%. Calcd for $C_{20}H_{17}N_3O_2$: C, 72.49; H, 5.17; N, 12.68%.

6. This was prepared in an analogous way to **5**, except for using EtOH instead of MeOH. (Dark red columnar crystals from benzene, 2.82 g, 85%), mp 175—177 °C. ^{1}H NMR δ_H = 1.41 (t, 3H, J = 7.2 Hz), 4.39 (q, 2H, J = 7.2 Hz), 7.05 (t, 1H), 7.25 (d, 2H, J = 8.8 Hz), 7.30 (d, 2H, J = 7.1 Hz), 7.36 (t, 2H, J = 6.6 Hz), 7.91 (d, 2H, J = 7.2 Hz), 7.94 (d, 2H, J = 6.6 Hz), 8.17 (d, 2H, J = 8.8 Hz), 8.23 (br s, 1H). IR (KBr) 3350, 1693, 1589, 1533, 1493,1429, 1392, 1348, 1286, 1236, 1134, 1097, 748, 696 cm^{-1}. HRMS (EI 70 eV) Found: *m/z* 345.1453. Calcd for $C_{21}H_{19}N_3O_2$: M, 345.1477. Found: C, 73.15; H, 5.69; N 12.18%. Calcd for $C_{21}H_{19}N_3O_2$: C, 73.03; H, 5.54; N, 12.17%.

7. A suspension of **4** (0.95 g, 3 mmol) and $SOCl_2$ (1.07 g, 9 mmol) in benzene (200 mL) was refluxed for 3 h. To the residue obtained by evaporating excess $SOCl_2$ and benzene were added 29% aqueous NH_3 (1.13 g, 20 mmol) and THF (200 mL), and the mixture refluxed for 1 h. After a white solid was removed by filtration, the solvent was evaporated to dryness. The resultant brown solid was washed with H_2O and chromatographed through silica gel (THF/$CHCl_3$ = 1/1). The second red band was isolated to afford an orange powdery solid (0.85 g, 86%), mp 225—226 °C. ^{1}H NMR δ_H = 6.73 (br s, 1H), 7.04 (t, 1H, J = 7.1 Hz), 7.25 (d, 2H, J = 8.8 Hz), 7.30 (d, 2H, J = 8.8 Hz), 7.36 (t, 2H, J = 7.2 Hz), 7.60 (br s, 1H), 7.90 (d, 4H, J = 8.6 Hz), 8.10 (d, 2H, J = 8.8 Hz), 8.18 (br s, 1H). IR (KBr) 3418, 3318, 3196, 1655, 1593, 1516, 1495, 1390, 1320, 1144, 862, 743, 695, 550, 492 cm^{-1}. HRMS (EI 70 eV) Found: *m/z* 316.1340. Calcd for $C_{19}H_{16}N_4O$: M, 316.1324.

8. To a stirred suspension of **7** (0.95 g, 3 mmol) in benzene (150 mL) at 50 °C was added P_2S_5 (0.13 g, 0.6 mmol) portionwise, and the mixture refluxed for 3 h. The reaction mixture was filtered and the insoluble residue was washed with benzene. The solvent was evaporated from the combined filtrate and the resulting red solid was chromatographed through silica (THF/$CHCl_3$ = 1/1). The second red band yielded a red powdery solid (0.10 g, 11%), mp 207—209 °C. ^{1}H NMR δ_H = 7.05 (t, 1H), 7.24 (d, 2H, J = 8.8 Hz), 7.30 (d, 2H, J = 8.1 Hz), 7.37 (t, 2H, J = 7.2 Hz), 7.86 (d, 2H, J = 8.8 Hz), 7.90 (d, 2H, J = 9.4 Hz), 8.16 (d, 2H, J = 8.3 Hz), 8.19 (br s, 1H), 9.03 (br s, 1H), 9.13 (br s, 1H). IR (KBr) 3382, 3276, 3154, 1626, 1590, 1512, 1312, 1142, 1130, 885, 855, 750 cm^{-1}. HRMS (EI 70 eV) Found: *m/z* 332.1121. Calcd for $C_{19}H_{16}N_4S$: M, 332.1095.

This work was partly supported by grants from the Research Foundation for Opto-Science and Technology and the Ministry of Education, Science, Sports and Culture, and by the High-Tech Research Center at Nihon University.

References

1 H. Rau, "Studies in Organic Chemistry 40: Photochromism: Molecules and Systems," ed by H. Dürr and H. Bouas-Laurent, Elsevier, Amsterdam (1990), Chap. 4, p. 165.

2 B. L. Feringa, W. F. Jager, and B. de Lange, *Tetrahedron*, **49**, 8267 (1993).

3 I. Willner and S. Rubin, *Angew. Chem., Int. Ed. Engl.*, **35**, 367 (1996).

4 A. Ueno, T. Kuwabara, A. Nakamura, and F. Toda, *Nature*, **356**, 136 (1992).

5 Z. F. Liu, B. H. Loo, R. Baba, and A. Fujishima, *Chem. Lett.*, **1990**, 1023.

6 Recently, we are exploring the use of azopyridine derivatives for photoelectrochemical molecular devices: a) J. Otsuki, K. Sato, M. Tsujino, N. Okuda, K. Araki, and M. Seno, *Chem. Lett.*, **1996**, 847. b) J. Otsuki, M. Tsujino, T. Iizaki, K. Araki, M. Seno, K. Takatera, and T. Watanabe, *J. Am. Chem. Soc.*, **119**, 7895 (1997). c) J. Otsuki, K. Harada, and K. Araki, *Chem. Lett.*, **1999**, 269.

7 B. J. Coe, *Chem. Eur. J.*, **5**, 2464 (1999).

8 P. D. Wildes, J. G. Pacifici, G. Irick, Jr., and D. G. Whitten, *J. Am. Chem. Soc.*, **93**, 2004 (1971).

9 J. Epperlein and B. Blau, *Z. Chem.*, **27**, 175 (1987).

10 a) T. Skarżyńska-Klentak and T. Widernik, *Pol. J. Chem.*, **53**, 989 (1979). b) T. Widernik and T. Skarżyńska-Klentak, *Pol. J. Chem.*, **53**, 1243 (1979). c) T. Widernik and T. Skarżyńska-Klentak, *Pol. J. Chem.*, **55**, 1759 (1981). d) A. Liwo, A. Tempczyk, T. Widernik, T. Klentak, and J. Czermiński, *J. Chem. Soc., Perkin Trans. 2*, **1994**, 71.

11 E. Sawicki, *J. Org. Chem.*, **22**, 1084 (1957).

12 G. M. Badger, R. G. Buttery, and G. E. Lewis, *J. Chem. Soc.*, **1954**, 1888.

13 E. Fischer and Y. Frei, *J. Chem. Phys.*, **27**, 328 (1957).

14 H. Bisle, M. Rómer, and H. Rau, *Ber. Bunsenges. Phys. Chem.*, **80**, 301 (1976).

15 I. Bridgeman and A. T. Peters, *J. Soc. Dyers Colourists*, **86**, 519 (1970).

16 V. Gutmann, "The Donor–Acceptor Approach to Molecular Interactions," Plemun, New York (1978).

17 G. Irick, Jr., and J. G. Pacifici, *Text. Res. J.*, **1972**, 391.

18 E. G. McRae, *J. Phys. Chem.*, **61**, 563 (1957).

19 a) N. Nishimura, T. Sueyoshi, H. Yamanaka, and E. Imai, *Bull. Chem. Soc. Jpn.*, **49**, 1381 (1976). b) T. Sueyoshi, N. Nishimura, S. Yamamoto, and S. Hasegawa, *Chem. Lett.*, **1974**, 1131.

20 M. T. Rogers, T. W. Campbell, and R. W. Maatman, *J. Am. Chem. Soc.*, **73**, 5122 (1951).
21 F. Gerson and E. Heilbronner, *Helv. Chim. Acta*, **45**, 51 (1962).
22 J. G. Calvert and J. N. Pitts, Jr., "Photochemistry," John Wiley & Sons, New York (1966), Chap. 7, p. 686.
23 "Aldrich Catalogue," Sigma-Aldrich (1998—1999), p. 1298.
24 E. Sawicki, *J. Org. Chem.*, **22**, 915 (1957).
25 M. D. Bhavsar and P. N. Saraiya, *Man-Made Textiles India*, **29**, 423 (1986).